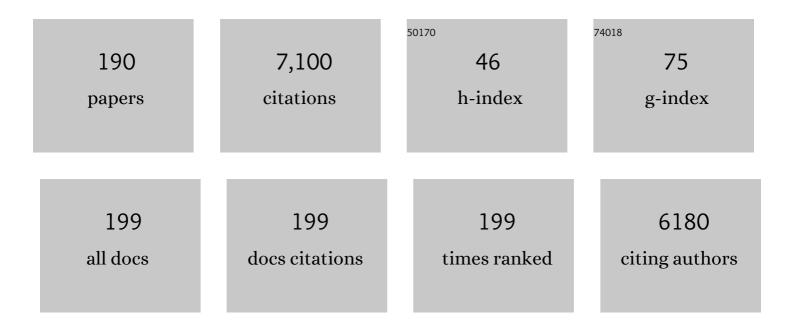
## Michael J Hoffmann

List of Publications by Year in descending order

Source: https://exaly.com/author-pdf/3575384/publications.pdf Version: 2024-02-01



#	Article	IF	CITATIONS
1	High capacity vertical aligned carbon nanotube/sulfur composite cathodes for lithium–sulfur batteries. Chemical Communications, 2012, 48, 4097.	2.2	282
2	Mechanisms of aging and fatigue in ferroelectrics. Materials Science and Engineering B: Solid-State Materials for Advanced Technology, 2015, 192, 52-82.	1.7	278
3	Nanodomain structure ofPb[Zr1â~'xTix]O3at its morphotropic phase boundary: Investigations from local to average structure. Physical Review B, 2007, 75, .	1.1	264
4	Lithium Diffusion Pathway in Li <sub>1.3</sub> Al <sub>0.3</sub> Ti <sub>1.7</sub> (PO <sub>4</sub> ) <sub>3</sub> (LATP) Superionic Conductor. Inorganic Chemistry, 2016, 55, 2941-2945.	1.9	188
5	Ferroelectric domains in methylammonium lead iodide perovskite thin-films. Energy and Environmental Science, 2017, 10, 950-955.	15.6	178
6	Direct comparison between hot pressing and electric field-assisted sintering of submicron alumina. Acta Materialia, 2009, 57, 5454-5465.	3.8	154
7	Sintering Model for Mixedâ€Oxideâ€Derived Lead Zirconate Titanate Ceramics. Journal of the American Ceramic Society, 1998, 81, 3277-3284.	1.9	143
8	Grain Boundary Films in Rareâ€Earthâ€Classâ€Based Silicon Nitride. Journal of the American Ceramic Society, 1996, 79, 788-792.	1.9	142
9	Nanodomains in morphotropic lead zirconate titanate ceramics: On the origin of the strong piezoelectric effect. Journal of Applied Physics, 2007, 102, .	1.1	128
10	Control of Lamellae Spacing During Freeze Casting of Ceramics Using Doubleâ€ <b>s</b> ide Cooling as a Novel Processing Route. Journal of the American Ceramic Society, 2009, 92, S79.	1.9	127
11	Grain Growth Studies of Silicon Nitride Dispersed in an Oxynitride Glass. Journal of the American Ceramic Society, 1993, 76, 2778-2784.	1.9	123
12	Development of a roadmap for advanced ceramics: 2010–2025. Journal of the European Ceramic Society, 2009, 29, 1549-1560.	2.8	123
13	Defect-Dipole Formation in Copper-Doped < mml:math xmlns:mml="http://www.w3.org/1998/Math/MathML" display="inline" > < mml:msub > < mml:mi > PbTiO < / mml:mi > < mml:mn > 3 < / mml:mn > < / mml:msub > < / mml:math > Ferroe Physical Review Letters, 2008, 100, 095504.	electrics.	118
14	Estimation of strain from piezoelectric effect and domain switching in morphotropic PZT by combined analysis of macroscopic strain measurements and synchrotron X-ray data. Acta Materialia, 2007, 55, 1849-1861.	3.8	107
15	Model experiments concerning abnormal grain growth in silicon nitride. Journal of the European Ceramic Society, 1996, 16, 3-14.	2.8	104
16	Temperature dependence of poling strain and strain under high electric fields in LaSr-doped morphotropic PZT and its relation to changes in structural characteristics. Acta Materialia, 2007, 55, 5780-5791.	3.8	96
17	Composition dependence of the domain configuration and size in Pb(Zr1â^'xTix)O3 ceramics. Journal of Applied Physics, 2007, 101, 074107.	1.1	93
18	Influence of Alkaline and Niobium Excess on Sintering and Microstructure of Sodiumâ€Potassium Niobate (K <sub>0.5</sub> Na <sub>0.5</sub> )NbO <sub>3</sub> . Journal of the American Ceramic Society, 2010, 93, 1270-1281.	1.9	90

#	Article	IF	CITATIONS
19	Influence of the Rare-Earth Element on the Mechanical Properties of RE-Mg-Bearing Silicon Nitride. Journal of the American Ceramic Society, 2005, 88, 2485-2490.	1.9	89
20	Ferroelectric Properties of Perovskite Thin Films and Their Implications for Solar Energy Conversion. Advanced Materials, 2019, 31, e1806661.	11.1	89
21	Sintering of in-Situ Synthesized Sic-TiB2 Composites with Improved Fracture Toughness. Journal of the American Ceramic Society, 1992, 75, 2479-2483.	1.9	85
22	Experimental evidence of the impact of rare-earth elements on particle growth and mechanical behaviour of silicon nitride. Materials Science & Engineering A: Structural Materials: Properties, Microstructure and Processing, 2006, 422, 66-76.	2.6	84
23	Universal Polarization Switching Behavior of Disordered Ferroelectrics. Advanced Functional Materials, 2012, 22, 2058-2066.	7.8	82
24	Electrical conductivity and stability of concentrated aqueous alumina suspensions. Journal of Colloid and Interface Science, 2005, 286, 579-588.	5.0	80
25	Development of Dense Fillerâ€Free Polymerâ€Derived SiOC Ceramics by Fieldâ€Assisted Sintering. Journal of the American Ceramic Society, 2008, 91, 3803-3805. <i>In situ</i> synchrotron diffraction investigation of morphotropic <mml:math< td=""><td>1.9</td><td>70</td></mml:math<>	1.9	70
26	xmlns:mml="http://www.w3.org/1998/Math/MathML" display="inline"> <mml:mrow> <mml:mi mathvariant="normal"&gt;Pb <mml:mrow> <mml:mo> [</mml:mo> <mml:msub> <mml:mi mathvariant="normal"&gt;Zr <mml:mrow> <mml:mn> 1 </mml:mn> <mml:mo> â^? </mml:mo> <mml:mi>x mathvariant="normal"&gt;Ti</mml:mi> <mml:mi>x </mml:mi> </mml:mrow></mml:mi </mml:msub> <mml:mo> ]</mml:mo> </mml:mrow> <mml:mrow> </mml:mrow>   ] </mml:mi </mml:mrow> <td>1.1 nml:mi&gt;&lt;, ml·msub&gt;</td> <td>/mml:mrow&gt;&lt;</td>	1.1 nml:mi><, ml·msub>	/mml:mrow><
27	mathvariant="normal">O. Physical Review B, 2007, 76, . Evolution of microstructure and its relation to ionic conductivity in Li1+xAlxTi2â^'x(PO4)3. Solid State Ionics, 2016, 288, 235-239.	1.3	68
28	Nonlinearity of strain and strain hysteresis in morphotropic LaSr-doped lead zirconate titanate under unipolar cycling with high electric fields. Journal of Applied Physics, 2007, 101, 044101.	1.1	67
29	Non-Arrhenius behavior of grain growth in strontium titanate: New evidence for a structural transition of grain boundaries. Scripta Materialia, 2015, 101, 68-71.	2.6	67
30	Slip Casting of SiC-Whisker-Reinforced Si3N4. Journal of the American Ceramic Society, 1989, 72, 765-769.	1.9	66
31	Characterization of ferroelectric domains in morphotropic potassium sodium niobate with scanning probe microscopy. Applied Physics Letters, 2007, 90, 252905.	1.5	66
32	The role of point defects and defect gradients in flash sintering of perovskite oxides. Acta Materialia, 2019, 165, 398-408.	3.8	65
33	An Overview of the Structure and Properties of Siliconâ€Based Oxynitride Glasses. International Journal of Applied Glass Science, 2011, 2, 63-83.	1.0	64
34	Three-dimensional organization of rare-earth atoms at grain boundaries in silicon nitride. Applied Physics Letters, 2005, 87, 061911.	1.5	62
35	Local variations in defect polarization and covalent bonding in ferroelectric Cu2+-doped PZT and KNN functional ceramics at the morphotropic phase boundary. Physical Chemistry Chemical Physics, 2009, 11, 8698.	1.3	62
36	Interactions of defect complexes and domain walls in CuO-doped ferroelectric (K,Na)NbO3. Applied Physics Letters, 2013, 102, .	1.5	62

#	Article	IF	CITATIONS
37	Structure and rheological properties of the RE–Si–Mg–O–N (RE=Sc, Y, La, Nd, Sm, Gd, Yb and Lu) glasses. Journal of Non-Crystalline Solids, 2004, 344, 8-16.	1.5	58
38	Electric Field-Assisted Sintering in Comparison with the Hot Pressing of Yttria-Stabilized Zirconia. Journal of the American Ceramic Society, 2011, 94, 24-31.	1.9	58
39	High strain lead-based perovskite ferroelectrics. Current Opinion in Solid State and Materials Science, 2004, 8, 51-57.	5.6	57
40	Correlation between Surface Texture and Chemical Composition in Undoped, Hard, and Soft Piezoelectric PZT Ceramics. Journal of the American Ceramic Society, 1998, 81, 721-724.	1.9	57
41	The equilibrium crystal shape of strontium titanate and its relationship to the grain boundary plane distribution. Acta Materialia, 2015, 82, 32-40.	3.8	54
42	Influence of Sr/Ti Stoichiometry on the Densification Behavior of Strontium Titanate. Journal of the American Ceramic Society, 2009, 92, 601-606.	1.9	52
43	On the importance of ferroelectric domains for the performance of perovskite solar cells. Nano Energy, 2018, 48, 20-26.	8.2	52
44	Short-Range and Medium-Range Order in Lithium Silicate Glasses, Part I: Diffraction Experiments and Results. Journal of the American Ceramic Society, 1996, 79, 2833-2838.	1.9	50
45	Iron-oxygen vacancy defect association in polycrystalline iron-modifiedPbZrO3antiferroelectrics: Multifrequency electron paramagnetic resonance and Newman superposition model analysis. Physical Review B, 2006, 73, .	1.1	48
46	Thermodynamic Calculations for the Formation of SiC-Whisker-Reinforced Si <sub>3</sub> N <sub>4</sub> Ceramics. Advanced Ceramic Materials, 1988, 3, 557-562.	2.3	48
47	Volume Expansion Caused by Water Penetration into Silica Glass. Journal of the American Ceramic Society, 2015, 98, 78-87.	1.9	47
48	Effect of Water Penetration on the Strength and Toughness of Silica Glass. Journal of the American Ceramic Society, 2011, 94, s196.	1.9	46
49	Substitution of Y2O3 by a rare earth oxide mixture as sintering additive of Si3N4 ceramics. Materials Letters, 2000, 45, 39-42.	1.3	44
50	Analysis of intrinsic lattice deformation in PZT-ceramics of different compositions. Journal of the European Ceramic Society, 2001, 21, 1349-1352.	2.8	43
51	Longâ€Term Behavior and Application Limits of Plasmaâ€5prayed Zirconia Thermal Barrier Coatings. Journal of the American Ceramic Society, 2001, 84, 1301-1308.	1.9	42
52	High-field/high-frequency EPR of paramagnetic functional centers in Cu2+- and Fe3+-modified polycrystalline Pb[ZrxTi1â^'x]O3 ferroelectrics. Magnetic Resonance in Chemistry, 2005, 43, S166-S173.	1.1	41
53	Formation of magnetic grains in ferroelectric Pb[Zr0.6Ti0.4]O3 ceramics doped with Fe3+ above the solubility limit. Applied Physics Letters, 2009, 94, 142901.	1.5	41
54	Growth of single crystalline seeds into polycrystalline strontium titanate: Anisotropy of the mobility, intrinsic drag effects and kinetic shape of grain boundaries. Acta Materialia, 2015, 95, 111-123.	3.8	41

#	Article	IF	CITATIONS
55	Grain growth in perovskites: What is the impact of boundary transitions?. Current Opinion in Solid State and Materials Science, 2016, 20, 286-298.	5.6	41
56	Water Penetration—Its Effect on the Strength and Toughness of Silica Glass. Metallurgical and Materials Transactions A: Physical Metallurgy and Materials Science, 2013, 44, 1164-1174.	1.1	39
57	Influence of temperature and upper cut-off voltage on the formation of lithium-ion cells. Journal of Power Sources, 2014, 264, 100-107.	4.0	39
58	Effect of the Amount of Additives and Postâ€Heat Treatment on the Microstructure and Mechanical Properties of Yttrium–α‧ialon Ceramics. Journal of the American Ceramic Society, 2003, 86, 2136-2142.	1.9	38
59	The influence of Mg substitution for Al on the properties of SiMeRE oxynitride glasses. Journal of Non-Crystalline Solids, 2004, 333, 124-128.	1.5	37
60	Characterization of (Fe <sub>Zr,Ti</sub> -V <sub>o</sub> <sup>ldrldr</sup> ) <sup>ldr</sup> defect dipoles in (La,Fe)-codoped PZT 52.5/47.5 piezoelectric ceramics by multifrequency electron paramagnetic resonance spectroscopy. IEEE Transactions on Ultrasonics, Ferroelectrics, and Frequency Control, 2008, 55, 1061-1068.	1.7	37
61	Defect structure and formation of defect complexes in Cu2+-modified metal oxides derived from a spin-Hamiltonian parameter analysis. Molecular Physics, 2009, 107, 1981-1986.	0.8	37
62	Solubility of Si <sub>3</sub> N <sub>4</sub> in Liquid SiO <sub>2</sub> . Journal of the American Ceramic Society, 2002, 85, 25-32.	1.9	36
63	Multifrequency electron paramagnetic resonance analysis of polycrystalline gadolinium-doped PbTiO3—Charge compensation and site of incorporation. Applied Physics Letters, 2006, 88, 122506.	1.5	36
64	Bipolar Fatigue Caused by Field Screening in Pb(Zr,Ti)O3Ceramics. Journal of the American Ceramic Society, 2007, 90, 070922001254005-???.	1.9	36
65	Grain growth transitions of perovskite ceramics and their relationship to abnormal grain growth and bimodal microstructures. Journal of Materials Science, 2016, 51, 1756-1765.	1.7	36
66	Processing and characterization of elastic and thermal expansion behaviour of interpenetrating Al12Si/alumina composites. Materials Science & Engineering A: Structural Materials: Properties, Microstructure and Processing, 2019, 743, 339-348.	2.6	36
67	Ferroelectric Poling of Methylammonium Lead Iodide Thin Films. Advanced Functional Materials, 2020, 30, 1908657.	7.8	36
68	Title is missing!. , 1998, 2, 75-84.		34
69	Contribution from Ferroelastic Domain Switching Detected Using Xâ€ray Diffraction to <i>R</i> urves in Lead Zirconate Titanate Ceramics. Journal of the American Ceramic Society, 2001, 84, 2921-2929.	1.9	34
70	Grain growth in weak electric fields in strontium titanate: Grain growth acceleration by defect redistribution. Journal of the European Ceramic Society, 2016, 36, 2773-2780.	2.8	34
71	Grain growth in strontium titanate in electric fields: The impact of spaceâ€charge on the grainâ€boundary mobility. Journal of the American Ceramic Society, 2019, 102, 3779-3790.	1.9	34
72	Electric Field-Assisted Sintering and Hot Pressing of Semiconductive Zinc Oxide: A Comparative Study. Journal of the American Ceramic Society, 2011, 94, 2344-2353.	1.9	33

#	Article	IF	CITATIONS
73	The mechanism of grain boundary motion in SrTiO3. Journal of Materials Science, 2016, 51, 467-475.	1.7	33
74	Influence of lanthanum doping on the morphotropic phase boundary of lead zirconate titanate. Journal of Applied Physics, 2010, 108, .	1.1	32
75	The effect of water penetration on crack growth in silica glass. Engineering Fracture Mechanics, 2013, 100, 3-16.	2.0	32
76	Preparation of Multipleâ€Cation alphaâ€SiAlON Ceramics Containing Lanthanum. Journal of the American Ceramic Society, 1999, 82, 229-232.	1.9	31
77	<i>R</i> â€Curve Determination for the Initial Stage of Crack Extension in Si <sub>3</sub> N <sub>4</sub> . Journal of the American Ceramic Society, 2008, 91, 3638-3642.	1.9	31
78	A comparison of power controlled flash sintering and conventional sintering of strontium titanate. Scripta Materialia, 2017, 130, 187-190.	2.6	31
79	Experimental measurement of stress at a four-domain junction in lead zirconate titanate. Journal of Applied Physics, 2005, 97, 094102.	1.1	30
80	Local symmetry-reduction in tetragonal (La,Fe)-codoped Pb[Zr <sub>0.4</sub> Ti <sub>0.6</sub> ]O <sub>3</sub> piezoelectric ceramics. Physica Scripta, 2007, T129, 12-16.	1.2	30
81	Effects of sintering temperature on microstructure and high field strain of niobium-strontium doped morphotropic lead zirconate titanate. Journal of Applied Physics, 2010, 107, 054111.	1.1	30
82	On the ferroelectricity of CH3NH3PbI3 perovskites. Nature Materials, 2019, 18, 1050-1050.	13.3	30
83	Processing and Elastic Property Characterization of Porous <scp><scp>SiC</scp></scp> Preform for Interpenetrating Metal/Ceramic Composites. Journal of the American Ceramic Society, 2012, 95, 3078-3083.	1.9	29
84	Sintering and grain growth in SrTiO <sub>3</sub> : impact of defects on kinetics. Journal of the Ceramic Society of Japan, 2016, 124, 346-353.	0.5	29
85	Probing the Microstructure of Methylammonium Lead Iodide Perovskite Solar Cells. Energy Technology, 2019, 7, 1800989.	1.8	29
86	Determination of functional center local environment in copper-modified Pb[Zr0.54Ti0.46]O3 ceramics. Journal of Applied Physics, 2004, 95, 8092-8096.	1.1	28
87	Microstructure of sodium-potassium niobate ceramics sintered under high alkaline vapor pressure atmosphere. Journal of the European Ceramic Society, 2014, 34, 4213-4221.	2.8	28
88	Chemical and structural effects on the high-temperature mechanical behavior of (1â^' <i>x</i> )(Na1/2Bi1/2)TiO3- <i>x</i> BaTiO3 ceramics. Journal of Applied Physics, 2015, 117, .	1.1	27
89	Fabrication and Characterization of Fully Inkjet Printed Capacitors Based on Ceramic/Polymer Composite Dielectrics on Flexible Substrates. Scientific Reports, 2019, 9, 13324.	1.6	27
90	Effect of drilling-induced damage on the open hole flexural fatigue of carbon/epoxy composites. Composite Structures, 2019, 215, 238-248.	3.1	27

#	Article	IF	CITATIONS
91	Densification Behavior and Properties of Y2O3-Containing alpha-SiAlON-Based Composites. Journal of the American Ceramic Society, 1996, 79, 1537-1545.	1.9	26
92	Preparation of βâ€Silicon Nitride Seeds for Selfâ€Reinforced Silicon Nitride Ceramics. Journal of the American Ceramic Society, 1999, 82, 1608-1610.	1.9	26
93	<i>R</i> Curves from Compliance and Optical Crack‣ength Measurements. Journal of the American Ceramic Society, 2010, 93, 2814-2821.	1.9	26
94	DEFECT STRUCTURE OF COPPER DOPED POTASSIUM NIOBATE CERAMICS. Functional Materials Letters, 2010, 03, 19-24.	0.7	26
95	Anti-thermal behavior of materials. Scripta Materialia, 2015, 103, 1-5.	2.6	26
96	Critical mechanical and electrical transition behavior of BaTiO3: The observation of mechanical double loop behavior. Journal of Applied Physics, 2012, 112, .	1.1	25
97	Grain size effects in donor doped lead zirconate titanate ceramics. Journal of Applied Physics, 2020, 128, .	1.1	25
98	CuO-doped NaNbO <mml:math <br="" xmlns:mml="http://www.w3.org/1998/Math/MathML">display="inline"&gt;<mml:msub><mml:mrow /&gt;<mml:mn>3</mml:mn></mml:mrow </mml:msub></mml:math> antiferroelectrics: Impact of aliovalent doping and nonstoichiometry on the defect structure and formation of secondary phases. Physical Review B, 2011,	1.1	24
99	84, . Anti-thermal grain growth in SrTiO3: Coupled reduction of the grain boundary energy and grain growth rate constant. Acta Materialia, 2018, 149, 11-18.	3.8	23
100	Effect of Water on the Inert Strength of Silica Glass: Role of Water Penetration. Journal of the American Ceramic Society, 2012, 95, 3847-3853.	1.9	21
101	Internal load transfer in an interpenetrating metal/ceramic composite material studied using energy dispersive synchrotron X-ray diffraction. Materials Science & Engineering A: Structural Materials: Properties, Microstructure and Processing, 2019, 753, 247-252.	2.6	21
102	Phase-field study of pore-grain boundary interaction. Journal of the Ceramic Society of Japan, 2016, 124, 329-339.	0.5	20
103	Short-Range and Medium-Range Order in Lithium Silicate Glasses, Part II: Simulation of the Structure by the Reverse Monte Carlo Method. Journal of the American Ceramic Society, 1996, 79, 2839-2846.	1.9	19
104	Transient Growth Bands in Silicon Nitride Cooled in Rareâ€Earthâ€Based Glass. Journal of the American Ceramic Society, 1997, 80, 1397-1404.	1.9	19
105	A reversible wetting transition in strontium titanate and its influence on grain growth and the grain boundary mobility. Acta Materialia, 2015, 101, 80-89.	3.8	19
106	Impact of the Intergranular Film Properties on Microstructure and Mechanical Behavior of Silicon Nitride. Key Engineering Materials, 2004, 264-268, 775-780.	0.4	18
107	Crack-Tip Toughness from Vickers Crack-Tip Opening Displacements for Materials with Strongly Rising R-Curves. Journal of the American Ceramic Society, 2011, 94, 1884-1892.	1.9	18
108	Homogenization of the thermoelastic properties of silicon nitride. Acta Materialia, 2011, 59, 6029-6038.	3.8	18

#	Article	IF	CITATIONS
109	Characterization of grain boundary disconnections in SrTiO3 part I: the dislocation component of grain boundary disconnections. Journal of Materials Science, 2019, 54, 3694-3709.	1.7	18
110	SiC-Ceramics with Tailored Porosity Gradients for Combustion Chambers. Key Engineering Materials, 2000, 175-176, 149-162.	0.4	16
111	Numerical Determination of the Effective Magnetic Path Length of a Single-Sheet Tester. IEEE Transactions on Magnetics, 2014, 50, 929-932.	1.2	16
112	Processing and Microstructural Evolution of Rare Earth Containing SiAlONs. Key Engineering Materials, 2003, 237, 141-148.	0.4	15
113	DEFECT STRUCTURE IN "SOFT" ( <font>Gd</font> , <font>Fe</font> )-CODOPED PZT 52.5/47.5 PIEZOELECTRIC CERAMICS. Functional Materials Letters, 2008, 01, 7-11.	0.7	15
114	Fatigue Crack Growth Behavior of Silicon Nitride: Roles of Grain Aspect Ratio and Intergranular Film Composition. Journal of the American Ceramic Society, 2013, 96, 259-265.	1.9	15
115	Characterization of Elastic Properties in Porous Silicon Carbide Preforms Fabricated Using Polymer Waxes as Pore Formers. Journal of the American Ceramic Society, 2013, 96, 2269-2275.	1.9	15
116	Different R-Curves for Two- and Three-Dimensional Cracks. International Journal of Fracture, 2008, 153, 153-159.	1.1	14
117	Method for the estimation of the total displacement of ferroelectric actuators under mixed thermal and electrical loading. Sensors and Actuators A: Physical, 2008, 144, 328-336.	2.0	14
118	Linking Grain Boundaries and Grain Growth in Ceramics. Advanced Engineering Materials, 2010, 12, 1230-1234.	1.6	14
119	<i>In situ</i> neutron diffraction study of electric field induced structural transitions in lanthanum doped lead zirconate titanate. Zeitschrift Für Kristallographie, 2011, 226, 155-162.	1.1	14
120	Phaseâ€ <scp>F</scp> ield Modeling of Diffusion Coupled Crack Propagation Processes. Advanced Engineering Materials, 2014, 16, 142-146.	1.6	14
121	Non-Arrhenius grain growth in strontium titanate: Quantification of bimodal grain growth. Acta Materialia, 2019, 174, 105-115.	3.8	14
122	HIGH ELECTRIC FIELD INDUCED STRAIN IN SOLID-STATE ROUTE PROCESSED BARIUM TITANATE CERAMICS. Functional Materials Letters, 2010, 03, 59-64.	0.7	13
123	Interaction of Modified ( <scp>K</scp> , <scp>Na</scp> NbO <sub>3</sub> Ceramics with <scp>Ag</scp> â€Containing Electrodes. Journal of the American Ceramic Society, 2011, 94, 3591-3595.	1.9	13
124	The mechanism of grain growth at general grain boundaries in SrTiO3. Scripta Materialia, 2020, 188, 206-211.	2.6	13
125	Sintering and microstructure of potassium niobate ceramics with stoichiometric composition and with potassium- or niobium excess. Journal of the European Ceramic Society, 2013, 33, 2127-2139.	2.8	12
126	Characterization of grain boundary disconnections in SrTiO3 Part II: the influence of superimposed disconnections on image analysis. Journal of Materials Science, 2019, 54, 3710-3725.	1.7	12

#	Article	IF	CITATIONS
127	Sinter-HIP of polymer-derived Al2O3–SiC composites with high SiC contents. Materials Letters, 2011, 65, 2462-2465.	1.3	11
128	A micromechanically motivated finite element approach to the fracture toughness of silicon nitride. Journal of the European Ceramic Society, 2013, 33, 1729-1736.	2.8	11
129	Sol-Gel Processing and Electrochemical Conversion of Inverse Spinel-Type Li2NiF4. Journal of the Electrochemical Society, 2015, 162, A679-A686.	1.3	11
130	Direct synthesis of trirutile-type LiMgFeF6 and its electrochemical characterization as positive electrode in lithium-ion batteries. Journal of Power Sources, 2015, 274, 1200-1207.	4.0	11
131	Tape casted thin films of solid electrolyte Lithium-Lanthanum-Titanate. Solid State Ionics, 2018, 328, 25-29.	1.3	11
132	Influence of PbO stoichiometry on the properties of PZT ceramics and multilayer actuators. Journal of the American Ceramic Society, 2019, 102, 5401-5414.	1.9	11
133	Estimation of the Highâ€Temperature <i>R</i> Curve for Ceramics from Strength Measurements Including Specimens with Focused Ion Beam Notches. Journal of the American Ceramic Society, 2010, 93, 2411-2414.	1.9	10
134	Double layer electrical conductivity as a stability criterion for concentrated colloidal suspensions. Colloids and Surfaces A: Physicochemical and Engineering Aspects, 2017, 520, 9-16.	2.3	10
135	The equilibrium crystal shape of strontium titanate: Impact of donor doping. Scripta Materialia, 2017, 127, 118-121.	2.6	10
136	Upscaling of LATP synthesis: Stoichiometric screening of phase purity and microstructure to ionic conductivity maps. Ionics, 2021, 27, 2017-2025.	1.2	10
137	Hard and Tough α-SiAION Ceramics. Materials Science Forum, 2000, 325-326, 219-224.	0.3	9
138	Low temperature sintering and high piezoelectric properties of strontium doped PNZT–PNN ceramics processed via the columbite route. Journal of the European Ceramic Society, 2007, 27, 3613-3617.	2.8	9
139	Determination of Subcritical Crack Growth Parameters in Polymerâ€Derived SiOC Ceramics by Biaxial Bending Tests in Water Environment. Journal of the American Ceramic Society, 2010, 93, 1540-1543.	1.9	9
140	Bimodal domain configuration and wedge formation in tetragonal Pb[Zr1â^'xTix]O3 ferroelectrics. Computational Materials Science, 2014, 81, 123-132.	1.4	9
141	Stressâ€Enhanced Swelling of Silica: Effect on Strength. Journal of the American Ceramic Society, 2016, 99, 2956-2963.	1.9	9
142	Uncovering the symmetry of the induced ferroelectric phase transformation in polycrystalline barium titanate. Journal of Applied Physics, 2021, 130, .	1.1	9
143	Phase Relationships in Neodymia and Ytterbia Containing SiAlONs. Key Engineering Materials, 2003, 237, 43-48.	0.4	8
144	Influence of Grain Size on the Tensile Creep Behavior of Ytterbiumâ€Containing Silicon Nitride. Journal of the American Ceramic Society, 2004, 87, 421-430.	1.9	8

#	Article	IF	CITATIONS
145	Microstructural development of Y-Î $\pm$ /(Î <sup>2</sup> )-sialons after post heat-treatment and its effect on mechanical properties. Ceramics International, 2004, 30, 229-238.	2.3	8
146	Thermodynamic Analysis of Grain Aspect Ratio in Fibrous Microstructures of Silicon Nitride. Journal of the American Ceramic Society, 1997, 80, 3250-3252.	1.9	8
147	Influence of crystal structure on crack propagation under cyclic electric loading in lead–zirconate–titanate. Journal of the European Ceramic Society, 2009, 29, 425-430.	2.8	8
148	Preparation of Transparent Glass Sponges via Replica Method using Highâ€Purity Silica. Journal of the American Ceramic Society, 2010, 93, 111-114.	1.9	8
149	Effect of damage by hydroxyl generation on strength of silica fibers. Journal of the American Ceramic Society, 2018, 101, 2724-2726.	1.9	8
150	Diffusion of water in silica: Influence of moderate stresses. Journal of the American Ceramic Society, 2018, 101, 1180-1190.	1.9	8
151	Influence of the A/B nonstoichiometry, composition modifiers, and preparation methods on properties of Li- and Ta-modified (K,Na)NbO3 ceramics. Journal of Applied Physics, 2012, 112, .	1.1	7
152	Diffusion of water in silica glass in the absence of stresses. Journal of the American Ceramic Society, 2017, 100, 3895-3902.	1.9	7
153	Control of the Surface Morphology of Ceramic/Polymer Composite Inks for Inkjet Printing. Advanced Engineering Materials, 2018, 20, 1800318.	1.6	7
154	Evolution of ferroelectric domains in methylammonium lead iodide and correlation with the performance of perovskite solar cells. Journal of Materials Chemistry A, 2021, 9, 21845-21858.	5.2	7
155	Processing and Properties of Coâ€Extruded Lead Zirconate Titanate Fibers. Journal of the American Ceramic Society, 2012, 95, 108-116.	1.9	6
156	Biaxial strength and slow crack growth in porous alumina with silica sintering aid. Journal of the European Ceramic Society, 2018, 38, 665-670.	2.8	6
157	A Novel Approach for the Processing of Advanced Polymer Derived Ceramics with Carbon Nanotubes with the Help of Pores. Advanced Engineering Materials, 2014, 16, 295-300.	1.6	5
158	The Impact of Heat Treatment on the Domain Configuration and Strain Behavior in Pb[Zr,Ti]O <sub>3</sub> Ferroelectrics. Journal of the American Ceramic Society, 2015, 98, 269-277.	1.9	5
159	Field Assisted Sintering of Nbâ€Al <sub>2</sub> O <sub>3</sub> Composite Materials and Investigation of Electrical Conductivity. Advanced Engineering Materials, 0, , .	1.6	5
160	Measuring Electrostatic Potential Profiles across Amorphous Intergranular Films by Electron Diffraction. Microscopy and Microanalysis, 2006, 12, 160-169.	0.2	4
161	Effect of intergranular glass on phase relation of Nd-α-sialon. Scripta Materialia, 2006, 54, 1469-1473.	2.6	4
162	Fatigue Threshold <i>R</i> urves Predict Fatigue Endurance Strength for Selfâ€Reinforced Silicon Nitride. Journal of the American Ceramic Society, 2014, 97, 577-583.	1.9	4

#	Article	IF	CITATIONS
163	Precursor derived SiOC/MoSi <sub>2</sub> -composites for diesel glow plugs: preparation and high temperature properties. Journal of the Ceramic Society of Japan, 2016, 124, 1017-1022.	0.5	4
164	Process Development for the Ceramic Injection Molding of Oxide Chopped Fiber Reinforced Aluminum Oxide. Key Engineering Materials, 0, 742, 231-237.	0.4	4
165	Powder Injection Molding of Oxide Ceramic CMC. Key Engineering Materials, 2019, 809, 148-152.	0.4	4
166	Devising a method of making actuators with reduced poling-induced tension. Sensors and Actuators A: Physical, 2003, 107, 14-20.	2.0	3
167	Lead Zirconate Titanate–Magnetoplumbite Composites: A First Step Toward Multiferroic Ceramics?. Journal of the American Ceramic Society, 2009, 92, 2362-2367.	1.9	3
168	A Residual Stress Intensity Factor Solution for Knoop Indentation Cracks. International Journal of Fracture, 2012, 175, 65-71.	1.1	3
169	Reduction of the Sintering Temperature for the Manufacturing of Carbonâ€Rich Dense SiOC Bulk Ceramics. Advanced Engineering Materials, 2018, 20, 1800369.	1.6	3
170	Development and characterization of half-cells based on thin solid state ionic conductors for Li-ion batteries. Solid State Ionics, 2019, 333, 66-71.	1.3	3
171	Interpreting rheology and electrical conductivity: It all boils down to which particle size. Journal of Colloid and Interface Science, 2020, 574, 97-109.	5.0	3
172	Influence of Grade of Agglomeration and Green Body Liquid Saturation on Bending Strength and Fracture Toughness of Slip-Cast Alumina. Key Engineering Materials, 2002, 206-213, 641-644.	0.4	2
173	Determination of Stability Areas of Yb- and Nd-α-SiAlON Phases Using the Rietveld Method. Key Engineering Materials, 2004, 264-268, 1075-1078.	0.4	2
174	Permittivity and loss tangent of unpoled LaSr-doped PZT under compressive loading. Journal of Materials Science, 2007, 42, 8753-8756.	1.7	2
175	Structural Characterization of Cu <sup>2+</sup> Functional Centers In â€~Lead-Free' KNN Piezoelectrics. Materials Research Society Symposia Proceedings, 2009, 1199, 7.	0.1	2
176	Influence of the A/B Stoichiometry on Defect Structure, Sintering, and Microstructure in Undoped and Cu-Doped KNN. , 2012, , 209-251.		2
177	Fabrication and High Temperature Creep Behaviour of Interpenetrated Nickel–Chromium/Alumina Composites. Advanced Engineering Materials, 2012, 14, 795-801.	1.6	2
178	Preparation of Optically Transparent Open elled Foams and its Morphological Characterization Employing Volume Image Analysis. Advanced Engineering Materials, 2011, 13, 1060-1065.	1.6	1
179	Identification of residual stress layers at glass surfaces via crack terminating angles. Journal of the American Ceramic Society, 2017, 100, 4173-4179.	1.9	1
180	Determination of <i>v</i> – <i>K</i> curves from lifetime tests with reloaded survivals. International Journal of Materials Research, 2008, 99, 1107-1112.	0.1	1

#	Article	IF	CITATIONS
181	Structural Analysis of Ceramic Suspensions by CRYO-SEM Investigations. , 2005, , 41-46.		0
182	Mode-II shielding-curve of Al2O3 from measurement of cone crack angles. Journal of Materials Science, 2008, 43, 2077-2081.	1.7	0
183	Effects of temperature on poling behavior and high field strain of morphotropic PZT. , 2008, , .		0
184	Failure of Alumina in Torsion Tests. Advanced Engineering Materials, 2010, 12, 942-947.	1.6	0
185	The Role of Binder Adsorption for High Solid Loading Nanoâ€Zirconia Extrusion Pastes. Journal of the American Ceramic Society, 2012, 95, 1901-1910.	1.9	0
186	Heat treatment effects on domain configuration and strain under electric field in undoped Pb[Zr <inf>x</inf> Ti <inf>1−x</inf> ]O <inf>3</inf> ferroelectrics. , 2013, , .		0
187	Ag-Migration in La-doped PZT-Multilayers. , 0, , 446-451.		0
188	Probing the Microstructure of Methylammonium Lead Iodide Solar Cells. , 2018, , .		0
189	Ferroelectric domains in methylammonium lead iodide perovskite solar cells. , 0, , .		0
190	Ferroelectric domains in methylammonium lead iodide perovskite solar cells. , 0, , .		0